

Influence of Injection Current on the internal quantum Efficiency of a-Si Quantum Dot's Light Emitting Diodes

Ass.prof.Dr. Moafak Cadim Abdulrida and Walaa Khalel Jameel*

Kut University College, Studies and Research Center

* College of Education for Pure Science University of Baghdad

Abstract

The internal quantum efficiency of amorphous silicon quantum dots (a-Si DQs), has been studied theoretically as a function of temperature and recombination lifetime of excited carriers. The increase in the internal quantum efficiency with decreasing QD size was attributed to the quantum confinement effects in a-Si QDs. This type of confinement has changed the optical energy gap of the material from indirect to nearly direct transition structure. It is found that the visible-light emission from a-Si QDs is most efficient at room temperature, and the efficiency increases with temperature and decreases with increasing recombination lifetime.

Keywords: Nano-LED, Quantum dots, a-Si, Quantum confinement.

تأثير تيار الحقن على الكفاءة الكمية الداخلية لثنائيات الإنبعاث الضوئي من النقاط الكمية للسليكون العشوائي

أ.م.د. موفق كاظم عبد الرضا
قسم هندسة الليزر والكهربوصرية
كلية الكوت الجامعة

ولاء خليل جميل*
كلية التربية للعلوم الصرفة (ابن الهيثم)
جامعة بغداد

لقد أجرينا دراسة نظرية الكفاءة الكمية الداخلية للنقاط الكمية من السليكون العشوائي بوصفها دالة على كل من درجة الحرارة وعمر بقاء إعادة الإتحاد لحوامل الشحنة المهيجة. إن الزيادة في الكفاءة الكمية الداخلية مع نقصان في حجم النقاط الكمية قد عزى أمره إلى تأثيرات التقيد الكمي والمكاني في النقاط الكمية للسليكون العشوائي. إذ أن هذا النوع من التقيد يغير فجوة الطاقة البصرية للمادة من غير مباشرة إلى مباشرة تقريبا. لقد وجد بأن الإنبعاث الضوئي البصري من مادة السليكون العشوائي ذا النقاط الكمية أكثر كفاءة عند درجة حرارة الغرفة وأن الكفاءة الكمية الداخلية تزداد مع درجة الحرارة وتقل بزيادة زمن عمر إعادة الإتحاد.

1. Introduction

Silicon-based light-emitting diodes (LEDs) represent promising candidates for the next generation of full-color and flat panel displays. The advantages of silicon-based LEDs include full-color emission, complementary metaloxide- semiconductor compatibility, system feasibility, and low cost of fabrication. Although a variety of emission colors from silicon, such as porous silicon and nanocrystalline silicon, Park et al. (2001) [1] show a sufficiently high efficiency that can be used in LED

applications, the tuning of emission color, particularly in the short wavelength region, continues to be a challenge. Quantum confinement effects (QCE) make silicon a likely candidate for full color displays [2], because the tuning of emission color and efficient emission can be achieved from the principle of confinements, whether special or quantum confinement.

Another important issue in realizing silicon-based LEDs is the operation voltage. Silicon oxide is typically used as a material for enclosing nano-sized silicon [3]. However, silicon oxide is a very large wide band gap insulator and, thus, results in a high operation voltage. Silicon nitride is a promising alternative material because it has lower barriers for electrons and holes than silicon oxide. Furthermore, amorphous silicon (*a*-Si) has two important advantages compared with bulk crystalline silicon: the luminescence efficiency in bulk *a*-Si is higher than that in crystalline silicon due to its structural disorder; and the band gap energy of bulk *a*-Si (1.6 eV) is larger than that of bulk crystalline silicon. As a result, *a*-Si represents a good candidate for short-wavelength luminescence. It would, therefore, be expected that these intrinsic advantages of *a*-Si and the quantum and special confinement effects in *a*-Si quantum dot (*a*-SiQD) could be used in silicon-based optoelectronic devices [4].

2. Structure and Theory

In this work we adopted the structure of Ni/Au contact on silicon nitride containing *a*-Si QDs to improve the light internal efficiency [1,2]. 38 nm silicon films containing *a*-Si QDs were grown by plasma enhanced vapor deposition (PECVD), in which nitrogen-diluted 5% SiH₄ and were used as the source of reactance. A lowly doped *p*-type Si wafer (100) with a hole concentration of about 10^{15} cm^{-3} was employed as a substrate. The Ni (9 nm)/Au (21 nm) contact deposited on the silicon nitride films was annealed in an air ambient for 80 sec. Amorphous Si QD LEDs with Ni/Au contact annealed at 400 °C in air was used. The forward voltage 8.5 V for the annealed Ni/Au contact, at input current annealed Ni/Au contact was drastically decreased by 5 V. The series resistance of the LED with annealed Ni/Au contact was also decreased. This is attributed to the decreased in resistance 2.46/sq for the annealed Ni/Au contact [4]. The energy gap (*E*) for three-dimensionally confined *a*-Si QD can be expressed as $E \text{ (eV)} = E_{\text{Bulk}} + c/d^2$ [5] based on an effective mass theory, where E_{Bulk} represent the bulk *a*-Si band gap, *d* the quantum dot size, and *c* is the confinement parameter. Fig (1) shows the structure of *a*-Si QD LED which has been adopted in this work.

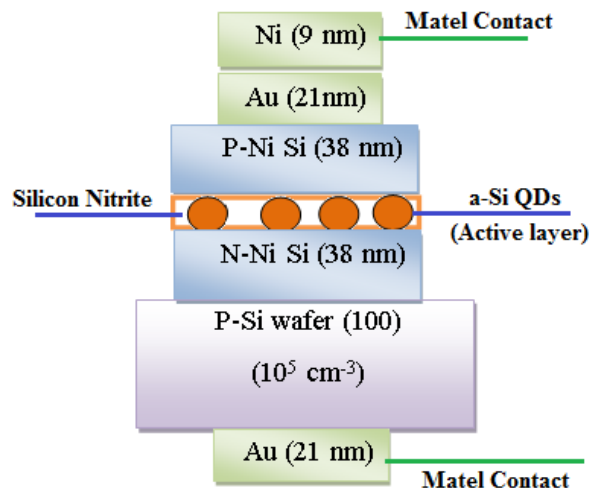


Fig (1): The structure of a-Si QDs LEDs which has been adopted

The internal quantum efficiency gauges what fractions of e-h recombination in the forward biased pn-junction are radiative and therefore lead to photon emission. Non-radiative transitions are those in which e-h recombine through a recombination center such as a crystal defect or an impurity and emit photons [6]. By definition,

$$\eta_{\text{int}} = \frac{\text{rate of radiative recombination}}{\text{total rate of recombination}} \quad (1)$$

The total rate of recombination whereas the number of photons emitted per second Φ_{ph} is determined by the rate of radiative recombination [7].

$$\eta_{\text{int}} = \frac{\Phi_{\text{ph}}}{I/e} \quad (2)$$

For parabolic electron-hole bands, the LED spontaneous emission rate can be written as: [8]:

$$r_{\text{sp}} = P_{\text{em}} N_j(E) e^{E/KT} \quad (3)$$

and after compensation the joint density of state in a zero dimensions system, the spontaneous emission rate written as:

$$r_{\text{sp}} = \frac{2}{\tau_r} \delta(E - E_{N1,N2,N3}) e^{E/KT} \quad (4)$$

the total photon flux emitted from the QDs LED can be obtained by integrating over r_{sp} , and from the properties of delta function the total photon flux is:

$$\Phi_{\text{ph}} = \frac{v}{\tau_r} e^{E/KT} \quad (5)$$

Where E the energy gap for three-dimensionally confined a-Si QDs, v is the volume of the active region and I_{inj} is injected current. Then compensate eq. (5) in eq. (2) we obtain:

$$\eta_{\text{int}} = 2 \frac{v}{\tau_r I_{\text{inj}}} e^{E/KT} \quad (6)$$

where, τ_r is the recombination lifetime.

3. Results and Discussion

Figs. (2) and (3), are the internal quantum efficiency η_{int} as a function of injection current at dot size 1.8 nm and different temperatures. Fig. (2) shows the internal quantum efficiency η_{int} as a function of injection current at $\tau_r = 11 \times 10^{-6}$ sec with dot size 1.8 [9]. It is found that, the increasing in internal quantum efficiency η_{int} with decreasing injection current, is higher than in temperature 200 K. In Fig. (3) it is observed that the internal quantum efficiency η_{int} increases with the decrease of injection. As well as, the internal quantum efficiency η_{int} at room temperature is higher than when $T = 200\text{K}$. But the internal quantum efficiency η_{int} in Fig. (3) at $\tau_r = 40\text{nsec}$ is higher than internal quantum efficiency η_{int} at $\tau_r = 11 \times 10^{-6}\text{sec}$ and of the same quantum dot size (1.8 nm).

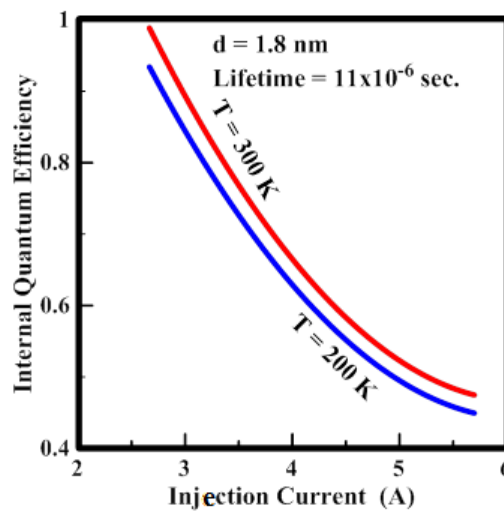


Fig (2): The internal quantum efficiency as a function of injection current at different temperatures with recombination lifetime 11×10^{-6} sec.

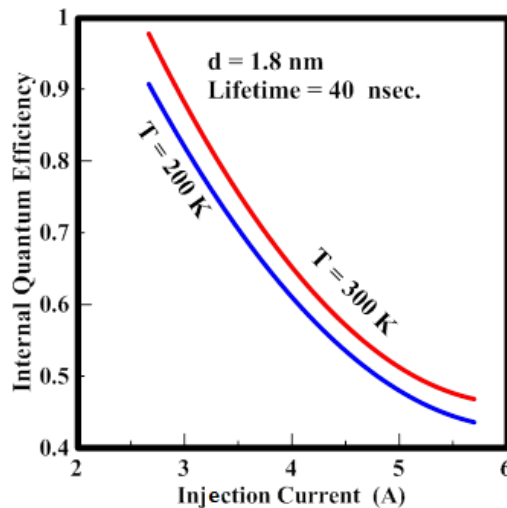


Fig (3): The internal quantum efficiency as a function of injection current at different temperatures with recombination lifetime 40nsec.

Figs. (4) and (5) show the internal quantum efficiency η_{int} as a function of injection current with different temperature and for lifetime 11×10^{-6} sec, at different dot size 1.8, 2.7 and 3.6 nm. It is clear, that the internal quantum efficiency η_{int} increases with decreasing injection current, in both figures. In Fig. (4), η_{int} is higher at the dot size 1.8 nm than dot size 2.7 and 3.6 nm, at room temperature and lifetime 11×10^{-6} sec. From Fig.(5), the internal quantum efficiency η_{int} when $T = 200$ K is highest at dot size 1.8 nm. In addition, the observed internal quantum efficiency η_{int} at dot size 2.7 and 3.6 nm is close together. Hence, the η_{int} at room temperature is higher than that when $T = 200$ K at different quantum dot size.

Fig (4): The internal quantum efficiency as a function of injection current at $T = 300$ K and lifetime is Equal to 11×10^{-6} sec.

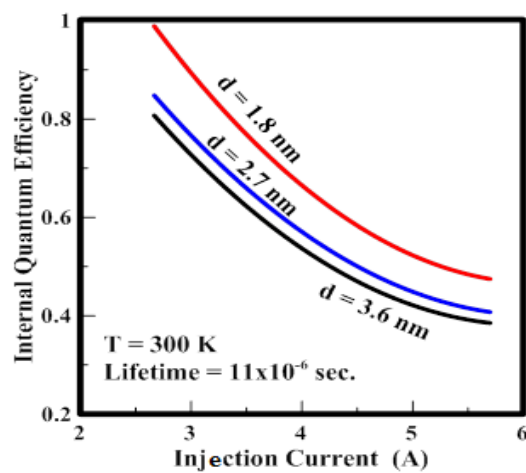
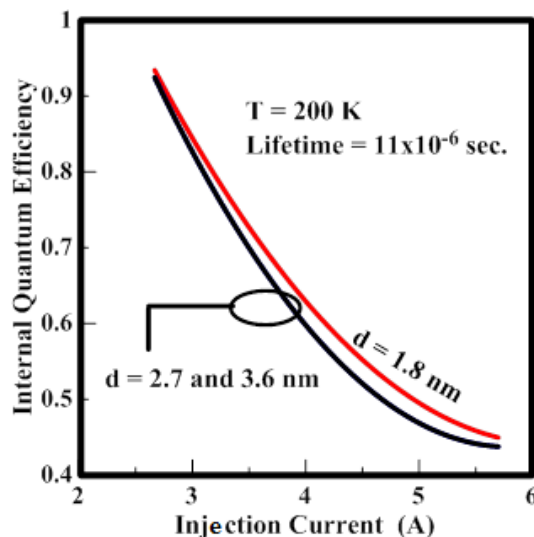


Fig (5): The internal quantum efficiency as a function of injection current at $T = 200$ K and lifetime is Equal to 11×10^{-6} sec.



Figs. (6) and (7) show the internal quantum efficiency η_{int} as a function of injection current at lifetime 40 nsec and different quantum dot size 1.8, 2.7 and 3.6 nm. In both figures the internal quantum efficiency η_{int} increases with the decreasing of injection current. From Fig. (6), the internal quantum efficiency η_{int} is close together at dot size 1.8 and 2.7 nm, and it is higher than dot size 3.6 nm. This result is at room temperature. From Fig. (7), the internal quantum efficiency η_{int} at dot size 1.8 and 2.7 nm is close to gather but at dot size 1.8 nm the internal quantum efficiency η_{int} is a bit

higher little. As well as, the internal quantum efficiency η_{int} at room temperature is higher than $T= 200$ K.

Fig (6): The internal quantum efficiency as a function of injection current with different dot size and at 300 K.

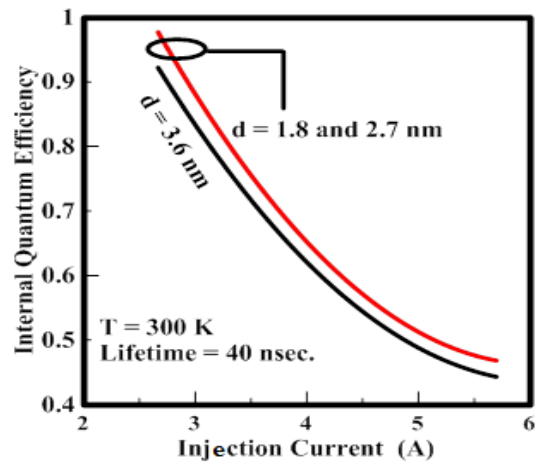
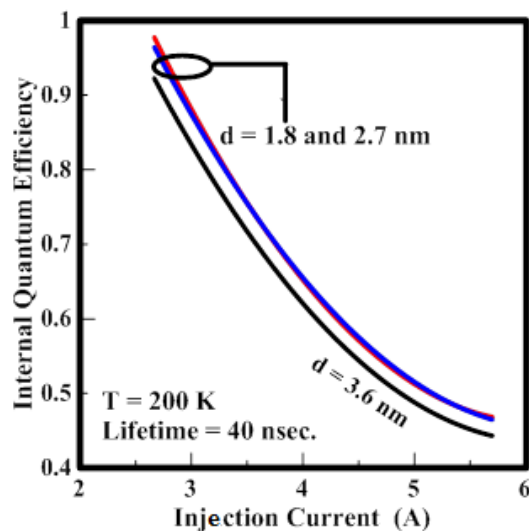


Fig (7): The internal quantum efficiency as a function of injection current with different dot size and at 200 K.



Figs. (8) and (9) show the internal quantum efficiency η_{int} as a function of injection current, at dot size 1.8 nm [9]. By observing both figures, the η_{int} increases with decreasing injection current. In Fig.(8), the internal quantum efficiency η_{int} at recombination lifetime 11×10^{-6} sec is higher than when $\tau_r = 40$ nsec at room temperature. Also the internal quantum efficiency, η_{int} , in Fig. (9), is the highest when lifetime 10×11^{-6} sec than $\tau_r = 40$ nsec at temperature 200 K. But the internal quantum efficiency η_{int} in both recombination lifetimes at room temperature is higher than internal quantum efficiency η_{int} at temperature 200 K.

Fig (8): The internal quantum efficiency as a function of injection current at different lifetime and at 300 K.

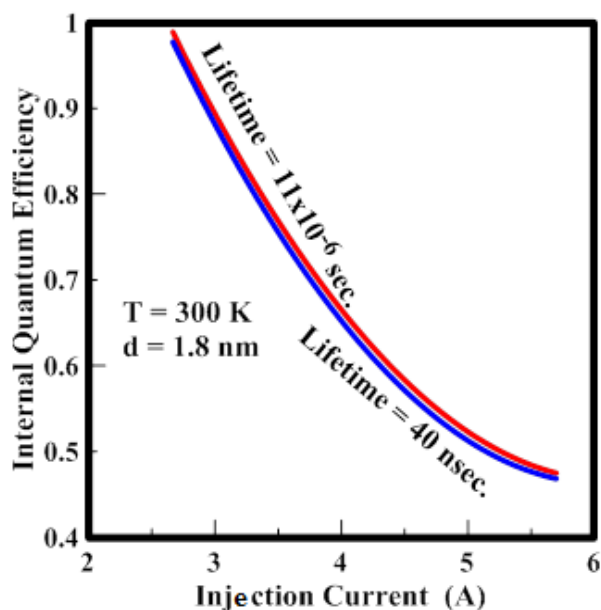
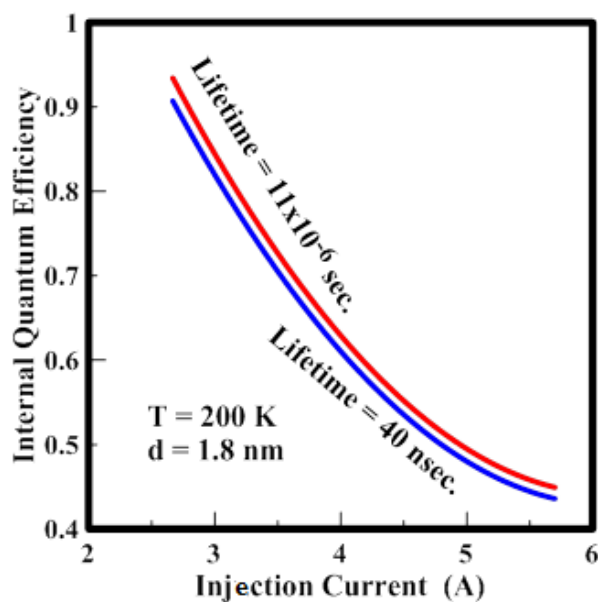


Fig (9): The internal quantum efficiency as a function of injection current at different lifetime and at 200 K.



The amorphous silicon QDs I n. The p- (Ni Si 38 nm) and n- (Ni Si 38 nm) layers act as the injectors of holes and electrons, respectively, into the luminescent a-Si QD region. In this kind of band structure, there are two possible processes for carrier injection into the a-Si QDs. If carriers have a higher thermal energy than the barrier height, they can flow over the barriers. This process is called as “thermionic emission.” This process would play only a minor role since the barrier heights at the p-a-Si and n-a-Si interfaces are much larger than the thermal energy of carriers at room temperature and consequently at 200K another process considered here is field-tunneling through the barriers under high electric field. In this case, the field-tunneling process will be considered as dominate injection current that flows in the a-Si QDs junction. The EL intensity is essentially proportional to the rate of the radiative recombination of electrons and

holes. The rate of the radiative recombination is in turn determined by the product of excess electron and hole densities at the initial and final states of the radiative transitions [10]. Therefore, the discussion to all the results of internal quantum efficiency as a function of injection current needs somehow more information, which will be considered in the future. But, the main point is how such material, which has been considered as indirect optical energy gap, could make a high radiative recombination transition probability? The answer for this point, hides behind the idea of quantum confinement. The dynamic of quantum confinement for *a-SiQDs* model is characterized by the shifting of energy levels for both conduction and valence bands. This shifting is proportional to the dot size, since the carriers are confined in three-dimensions, which is the case of quantum dots. This leads to the overlap of the envelope wave functions, which is more than in the other nanostructures. However, the shifting of energy levels becomes more when the dot size decreases. This can be explained by:- As the dot size decreases the effective mass of electron (hole) decreases (increases), therefore; the energy levels are shifted to higher (lower) magnitude of conduction (valence) band, which results from the assumption of $\left(\frac{1}{m^*} = \frac{1}{m_e} + \frac{1}{m_h^*}\right)$. For this reason, the energy gap has different values depending on the dot size. By applying Bohr's law in this case, the photon energy for each size has unique value, where it increases as the dot size decreases (*blue shifting*). In fact, the origin of quantum confinement is known to arise from the spatial confinement of carriers within the quantum dot boundary [11]. This means that the spatial confinement coexists with the quantum confinement. Since the spatial confinement of carriers inside a quantum dot is the reflecting or the folding of phonons in the k-space when the dot size decreases, the energy levels will shift to higher (lower) magnitude for conduction (valence) band by the quantum confinement. This relaxes the

4. Conclusions

In this work, a-Si light emitting diode quantum dots are designed. The most important conclusions from this work are:

At room temperature, the internal quantum efficiency shows more efficient than temperature 200 k.

The quantum confinement makes to shift the photoluminescence into visible region (blue shift) by controlling the dot size of a-SiQDs. From this behavior and the quantum efficiency, it is led to the performance that the a-SiQDs material has been changed to be direct band gap material. In fact, it is difficult to inject electrical carriers into a-SiQDs through the insulating silicon nitride film, although a-SiQDs embedded in silicon nitride film, so to increase the internal quantum efficiency Ni/Au contact was put on silicon nitride containing a-SiQDs in an attempt to improve the injection current.

The internal quantum efficiency increases with decreasing the injection current, and readily decreases when injection current increases. The temperature and recombination

lifetime affect the quantum efficiency. The quantum dots size, affects the internal quantum efficiency, since, whenever the dot sizes decrease the quantum efficiency increases and vice versa.

Acknowledgement

We would like to give our thanks to Dr. Ahlam H. Al Musawi for her fruitful discussion.

References

1. Park, N. M., Kim, T-S., and Park, S-J., (2001), "Band gap engineering of amorphous silicon quantum dots for light-emitting diodes", Vol. 78, No. 17, pp: 2575,.
2. Park, N. M., Choi, C. J., Seong T. Y., and Park, S. J., (2001a), Phys. Rev. Lett. 86, 1355.
3. Park, N. M., Kim, S. H., Sung, G. Y., and Park, S. J., (2002), Chem. Vap. Deposition **8**, 254.
4. Park, N. M., and Sung, G. Y., (2006), "Ni/Au contact to silicon quantum dot light-emitting diodes for the enhancement of the carrier injection and light extraction efficiency", Appl. Phys. Lett., Vol. 89, No. 063509, pp: 063509-1,5.
5. Kim, T. W., Cho, C. H., Kim, B. H., and Park, S. J., (2006), Appl. Phys. Lett. **88**, 123102.
6. Helm, M., and Dekorsy, T., (2009), " silicon based microcavity enhanced light emitting diodes", Ch. 2, Section, (2.2.4),.
7. Manasreh, O., (2005), "Semiconductor Hetero junctions and Nano- structures", McGraw-Hill,.
8. T.S. Moss, "Optical Properties of Semiconductors "Academic Press INC., New York, (1995).
9. T. W. Kim, C. H. Cho, B. H. Kim, and S. J. Park, Appl. Phys. Lett. **88**, 123102 (2006).
10. Hongping Zhao, Guangyu Liu, Jing Zhang, Ronald A. Arif, and Nelson Tansu, Journal of Display Technology, **9**, No. **4**, (2013).
11. M. Zhou, and I. Ghosh, Piptide Science, **88**, No. **3**, pp: 325-339 (2006).